

Discrete Boltzmann model of shallow water equations with polynomial equilibria

Jianping Meng*, Xiao-Jun Gu, David R Emerson
Scientific Computing Department, STFC Daresbury laboratory,
Warrington WA4 4AD, United Kingdom

Yong Peng†, Jianmin Zhang
State Key Laboratory of Hydraulics and Mountain River Engineering,
Sichuan University, Chengdu, 610065, P. R. China

October 4, 2021

Abstract

A type of discrete Boltzmann model for simulating shallow water flows is derived by using the Hermite expansion approach. Through analytical analysis, we study the impact of truncating distribution function and discretizing particle velocity space. It is found that the convergence behavior of expansion is nontrivial while the conservation laws are naturally satisfied. Moreover, the balance of source terms and flux terms for steady solutions is not sacrificed. Further numerical validations show that the capability of simulating supercritical flows is enhanced by employing higher order expansion and quadrature.

Keywords: Discrete Boltzmann model, Shallow water equations, Supercritical flows

1 Introduction

There is significant interest in modeling shallow water flows at mesoscopic level [1, 2, 3, 4, 5, 6, 7], in particular developing the lattice Boltzmann model (LBM) [5, 6, 7]. The LBM can be considered as a special discrete velocity method (DVM) for which a minimal discrete velocity set¹ is sought and tied to the discretization in space [8]. In this way, the LBM is sufficiently simple yet powerful enough to handle complex flow problems, and gradually gains popularity.

A critical challenge for LBM is to simulate supercritical shallow water flows characterized by a high Froude (Fr) number. For this purpose, an asymmetric model is proposed in [9] for simulating one-dimensional flows with $Fr > 1$. La Rocca et al. [10], has recently proposed a multi-speed model by matching hydrodynamic moments and successfully simulated both one-dimensional and two-dimensional supercritical flows. Since the discrete velocities are not integer in general, a finite difference scheme has to be used so that the model is best classified as a discrete Boltzmann model (DBM) or DVM. However, this model only partially recovers the original simplicity of the LBM.

The previous works have mainly been achieved by applying the approach of matching hydrodynamic moments [5, 6, 7, 10]. Inspired by these successes, in particular on the supercritical flows [10], we will investigate the Hermite expansion approach [11, 12] in this work, which is another major approach of seeking optimal DBMs. By using this approach, we are able to derive a range of discrete Boltzmann models with polynomial equilibria (DBMPE). Due to the property of the approach, both integer and non-integer discrete velocity sets can be obtained, and we can have the flexibility of choosing either the stream-collision scheme or general finite difference schemes for simulations. Specifically, the efficient lattice Boltzmann scheme is realised by using the stream-collision scheme. The order of

*Corresponding author.

†Jianping Meng and Yong Peng contributed equally to this work and should be considered as co-first authors.

¹Since a discrete velocity set is often obtained from a quadrature for integration, we consider these two terminologies exchangeable here. In particular, if the discrete velocities are integer numbers, the terminology “lattice” is also used.

expansion may also be tuned according to the Froude number of the flow. Typically, a second-order expansion is suitable for subcritical flows and a high-order expansion is necessary for supercritical flows. We will discuss the impact of expansion order on the accuracy as well as the well-balancing property of derived DBMs.

2 Discrete Boltzmann model with polynomial equilibria

2.1 Derivation

If the vertical length scale is much less than the horizontal length scale, the water flows are dominated by the nearly horizontal motion and are referred as shallow water flows. For these flows, the shallow water equations (SWEs) are employed to simplify the modeling, which are written as [13]

$$\frac{\partial h}{\partial t} + \nabla \cdot (h\mathbf{V}) = 0 \quad (1)$$

and

$$\frac{D\mathbf{V}}{Dt} = \frac{\partial \mathbf{V}}{\partial t} + \mathbf{V} \cdot \nabla \mathbf{V} = -\frac{1}{h} \nabla \mathcal{P} + \mathbf{F} + \nabla \cdot \boldsymbol{\sigma}, \quad (2)$$

where

$$\nabla \cdot \boldsymbol{\sigma} = \nu \nabla \cdot [\nabla \mathbf{V} + (\nabla \mathbf{V})^T - (\nabla \cdot \mathbf{V})\boldsymbol{\delta}] \approx \nu \Delta \mathbf{V},$$

and $\boldsymbol{\delta}$ (i.e., δ_{ij}) is the unit tensor. The equations describe the evolution of depth, h , and depth-averaged velocity, $\mathbf{V} = (u, v)$. The flows are often driven by a body force, \mathbf{F} , which represents not only the effects of an actual body force, including geostrophic force and tide-raising forces, but also those of wind stress, surface slope and atmospheric pressure gradient. The pressure

$$\mathcal{P} = \frac{gh^2}{2} \quad (3)$$

originates from the hydrostatic assumption, where g represents for the gravitational acceleration. If necessary, the viscous term $h\nu\Delta\mathbf{V}$ may also be considered where ν is the depth averaged kinematic viscosity. As has been shown, the SWEs are mathematically analogous to the two-dimensional compressible flow equations. In fact, they may be considered as a system of describing an ideal gas with the state equation Eq. (3), the ratio of specific heat $\gamma = 2$, and the ‘‘sound speed’’ \sqrt{gh} (cf. Chapter 2.1 in [13]).

A Boltzmann-BGK type equation can then be constructed for modeling SWEs [1],

$$\frac{\partial f}{\partial t} + \mathbf{c} \cdot \frac{\partial f}{\partial \mathbf{r}} + \mathbf{F} \cdot \frac{\partial f}{\partial \mathbf{c}} = \frac{f^{eq} - f}{\tau} \quad (4)$$

where

$$f^{eq} = \frac{1}{\pi g} \exp\left[\frac{(\mathbf{c} - \mathbf{V}) \cdot (\mathbf{c} - \mathbf{V})}{gh}\right]. \quad (5)$$

At the mesoscopic scale, the evolutionary variable becomes the distribution function $f(\mathbf{r}, \mathbf{c}, t)$ which represents the number of particles in the volume $d\mathbf{r}$ centered at position $\mathbf{r} = (x, y)$ with velocities within $d\mathbf{c}$ around velocity $\mathbf{c} = (c_x, c_y)$ at time t . The macroscopic quantities can be obtained by integrating over the whole particle velocity space, i.e.,

$$h = \int f d\mathbf{c} = \int f^{eq} d\mathbf{c}, \quad (6)$$

$$h\mathbf{V} = \int f \mathbf{c} d\mathbf{c} = \int f^{eq} \mathbf{c} d\mathbf{c}, \quad (7)$$

and

$$2\mathcal{P} = hgh = \int f(\mathbf{c} - \mathbf{V}) \cdot (\mathbf{c} - \mathbf{V}) d\mathbf{c}. \quad (8)$$

Moreover, the right-hand side (RHS) term of Eq. (4) obeys the conservation property of the collision integral as shown in Eqs. (6) and (7). Similar to an actual ideal gas, the relation between the relaxation time and kinetic viscosity is

$$\nu h = \mathcal{P}\tau, \quad (9)$$

which can be obtained by using the Chapman-Enskog expansion.

In principle, this kinetic equation may be solved directly by using regular numerical discretization for both physical space and particle velocity space, i.e., the DVM. Compared with direct discretization of SWEs, there are two more degrees of freedom for the particle velocity, which need to be treated carefully for both accuracy and efficiency. Among various schemes, the Gauss-type quadrature can provide a very efficient yet simple to implement discretization if properly truncating the equilibrium function Eq. (5), i.e., the Hermite expansion approach [14, 11, 12]. In this work, we shall derive a type of discrete Boltzmann models for shallow water flows using this approach. For this purpose, it is convenient to first introduce a non-dimensional system,

$$\begin{aligned} \hat{\mathbf{r}} &= \frac{\mathbf{r}}{h_0}, \hat{\mathbf{V}} = \frac{\sqrt{2}\mathbf{V}}{\sqrt{gh_0}}, \hat{t} = \frac{\sqrt{gh_0}t}{\sqrt{2}h_0}, \hat{\mathbf{F}} = 2\frac{\mathbf{F}}{g}, \\ \hat{\mathbf{c}} &= \frac{\sqrt{2}\mathbf{c}}{\sqrt{gh_0}}, \hat{f} = f\frac{g}{2}, \hat{\nu} = \frac{\nu}{\nu_0}, \hat{h} = \frac{h}{h_0}, \hat{\mathcal{P}} = \frac{\mathcal{P}}{\mathcal{P}_0} = \hat{h}^2, \end{aligned} \quad (10)$$

where the hat symbol denotes the non-dimensional variables. The reference depth, h_0 , can be the characteristic depth of the system such as the initial depth at the inlet (e.g., h_l in Fig. 2), while the reference viscosity is represented by ν_0 and the reference pressure \mathcal{P}_0 is chosen as $gh_0^2/2$. By using these non-dimensional variables, Eqs. (4) and (5) become,

$$\frac{\partial \hat{f}}{\partial \hat{t}} + \hat{\mathbf{c}} \cdot \frac{\partial \hat{f}}{\partial \hat{\mathbf{r}}} + \hat{\mathbf{F}} \cdot \frac{\partial \hat{f}}{\partial \hat{\mathbf{c}}} = \frac{\mathcal{P}_0}{\nu_0 \sqrt{gh_0/2}} \frac{\hat{\mathcal{P}}}{\hat{\nu} \hat{h}} (\hat{f}^{eq} - \hat{f}), \quad (11)$$

and

$$\hat{f}^{eq} = \frac{1}{2\pi} \exp\left[-\frac{(\hat{\mathbf{c}} - \hat{\mathbf{V}}) \cdot (\hat{\mathbf{c}} - \hat{\mathbf{V}})}{2\hat{h}}\right], \quad (12)$$

while there is no need to change the form of Eqs. (6) - (8). We may also define a ‘‘Knudsen’’ number

$$\mathcal{K} = \frac{\nu_0 \sqrt{gh_0/2}}{\mathcal{P}_0} = \frac{\nu_0 \sqrt{gh_0/2}}{gh_0^2/2}, \quad (13)$$

and the local Froude number becomes

$$Fr = \frac{U}{\sqrt{gh}} = \frac{\hat{U} \sqrt{gh_0/2}}{\sqrt{g\hat{h}h_0}} = \frac{\hat{U}}{\sqrt{2\hat{h}}}, \quad (14)$$

where the velocity magnitude is denoted by U . Using the ‘‘Knudsen’’ number and the fact that the viscosity is often considered as a constant, the RHS term of Eq.(11) becomes,

$$\frac{\hat{h}}{\mathcal{K}} (\hat{f}^{eq} - \hat{f}).$$

Hence, the actual relaxation time may change with time locally. Hereinafter, we shall use the non-dimensional version of quantities and equations by default, and the hat symbol will be omitted for clarity. It is also convenient to use the symbol τ to substitute for \mathcal{K}/\hat{h} in writing the equations.

First of all, the equilibrium distribution will be expanded on the basis of the Hermite orthogonal polynomials $\chi^{(n)}(\mathbf{c})$ in particle velocity space (see Ref. [11] for detail), i.e.,

$$f^{eq} \approx f_{eq}^N = \omega(\mathbf{c}) \sum_{n=0}^N \frac{1}{n!} \mathbf{a}_{eq}^{(n)} : \chi^{(n)}(\mathbf{c}), \quad (15)$$

where the N^{th} order terms are retained and the full contraction of tensors are denoted by the symbol $:$. The coefficient $\mathbf{a}_{eq}^{(n)}$ is given by

$$\mathbf{a}_{eq}^{(n)} = \int f^{eq} \boldsymbol{\chi}^{(n)} d\mathbf{c} \cong \sum_{\alpha=1}^d \frac{w_{\alpha}}{\omega(\mathbf{c}_{\alpha})} f_{eq}^N \boldsymbol{\chi}^n(\mathbf{c}_{\alpha}). \quad (16)$$

Using the Gauss-Hermite quadrature with weights w_{α} and abscissae \mathbf{c}_{α} , $\alpha = 1, \dots, d$, the integration in Eq. (16) has been converted into a summation. In particular, the exact equality holds if a sufficient order of quadrature is employed [11]. The first few coefficients are given by

$$\mathbf{a}_{eq}^{(0)} = h, \quad (17)$$

$$\mathbf{a}_{eq}^{(1)} = h\mathbf{V}, \quad (18)$$

$$\mathbf{a}_{eq}^{(2)} = h[\mathbf{V}^2 + (h-1)\boldsymbol{\delta}], \quad (19)$$

$$\mathbf{a}_{eq}^{(3)} = h[\mathbf{V}^3 + (h-1)\boldsymbol{\delta}\mathbf{V}], \quad (20)$$

and

$$\mathbf{a}_{eq}^{(4)} = h[\mathbf{V}^4 + (h-1)\boldsymbol{\delta}\mathbf{V}^2 + (h-1)^2\boldsymbol{\delta}^2], \quad (21)$$

where the product of two tensors means the sum of all possible permutations of tensor product (e.g., $\boldsymbol{\delta}\mathbf{V} = V_i\delta_{jk} + V_j\delta_{ik} + V_k\delta_{ij}$) while the power of a vector stands for the direct velocity product (e.g., $\mathbf{V}^3 = \mathbf{V}\mathbf{V}\mathbf{V}$). It is easy to verify that, with an appropriate quadrature, the conservation property of the collision integral will be satisfied automatically using an expansion higher than the first order, which will simplify the algorithm. The body force term $\mathcal{F}(\mathbf{x}, \mathbf{c}, t) = -\mathbf{F} \cdot \nabla_{\mathbf{c}} f$ can also be approximated as,

$$\mathcal{F}(\mathbf{x}, \mathbf{c}, t) = \omega(\mathbf{c}) \sum_{n=1}^N \frac{1}{(n-1)!} \mathbf{F}\mathbf{a}^{(n-1)} : \boldsymbol{\chi}^{(n)}, \quad (22)$$

where $\mathbf{a}^{(n)}$ is the corresponding coefficients for the distribution function, f . The first two are same as the \mathbf{a}_{eq}^0 and $\mathbf{a}_{eq}^{(1)}$ while the higher order terms can be related to stress and heat flux. Through the expansion, the kinetic equation (11) can be rewritten in its truncated form, i.e.,

$$\frac{\partial f}{\partial t} + \mathbf{c} \cdot \frac{\partial f}{\partial \mathbf{r}} = -\frac{1}{\tau}(f - f_{eq}^N) + \mathcal{F}. \quad (23)$$

Thus, we will be solving an approximation of the original kinetic equation.

The second step is to discretize Eq. (23) in the particle velocity space. The Gauss-Hermite quadrature is a natural choice. In one dimension, the discrete velocities c_{α} are just the roots of Hermite polynomials, and the corresponding weights are determined by:

$$w_{\alpha} = \frac{n!}{[n\chi^{n-1}(c_{\alpha})]^2}. \quad (24)$$

Given one-dimensional velocity sets, those of a higher-dimension can be constructed using the ‘‘production’’ formulae [11]. Once the discrete velocity set is chosen, the governing equation is discretized as

$$\frac{\partial f_{\alpha}}{\partial t} + \mathbf{c}_{\alpha} \cdot \frac{\partial f_{\alpha}}{\partial \mathbf{r}} = -\frac{1}{\tau}(f_{\alpha} - f_{\alpha}^{eq}) + \mathcal{F}_{\alpha}, \quad (25)$$

where $f_{\alpha} = w_{\alpha} f(\mathbf{r}, \mathbf{c}_{\alpha}, t) / \omega(\mathbf{c}_{\alpha})$, $f_{\alpha}^{eq} = w_{\alpha} f_{eq}^N(\mathbf{r}, \mathbf{c}_{\alpha}, t) / \omega(\mathbf{c}_{\alpha})$ and $\mathcal{F}_{\alpha} = w_{\alpha} \mathcal{F}(\mathbf{r}, \mathbf{c}_{\alpha}, t) / \omega(\mathbf{c}_{\alpha})$. According to Eqs. (17) - (21) and (15), the explicit form of the fourth order, f_{α}^{eq} , is

$$\begin{aligned} f_{\alpha}^{eq} = & h w_{\alpha} (1 + c_i V_i + \frac{1}{2}((c_i V_i)^2 - V_i V_i + (h-1)(c_i c_i - 2)) \\ & + \underbrace{\frac{c_i V_i}{6}((c_i V_i)^2 - 3V_i V_i + 3(h-1)(c_i c_i - 4))}_{\text{3rd}}, \\ & \left. \begin{aligned} & + \frac{1}{24}((c_i V_i)^4 - 6(V_i c_i)^2 V_j V_j + 3(V_j V_j)^2) \\ & + \frac{h-1}{4}((c_i c_i - 4)((V_i c_i)^2 - V_i V_i) - 2(V_i c_i)^2) \\ & + \frac{(h-1)^2}{8}((c_i c_i)^2 - 8c_i c_i + 8) \end{aligned} \right\} \text{4th} \end{aligned} \quad (26)$$

where the third order and the fourth order terms are highlighted.

We have now obtained the DBMPE (25). To conduct a numerical simulation, however, the physical space \mathbf{r} and the time t are needed to be discretized. For this purpose, any available schemes may be utilized according to the property of flow, such as finite difference/volume/element schemes. In particular, if using abscissae consisting of integers, the lattice Boltzmann scheme

$$\tilde{f}_\alpha(\mathbf{r} + \mathbf{c}_\alpha dt, t + dt) - \tilde{f}_\alpha(\mathbf{r}, t) = -\frac{dt}{\tau + 0.5dt} \left[\tilde{f}_\alpha(\mathbf{r}, t) - f_\alpha^{eq}(\mathbf{r}, t) \right] + \frac{\tau \mathcal{F}_\alpha dt}{\tau + 0.5dt} \quad (27)$$

can be constructed by introducing

$$\tilde{f}_\alpha = f_\alpha + \frac{dt}{2\tau} (f_\alpha - f_\alpha^{eq}) - \frac{dt}{2} \mathcal{F}_\alpha,$$

which allows the stream-collision scheme. Due to this unique property, the LBM has attracted significant interests in broad areas including shallow water simulations. However, if a high-order expansion is used, the abscissae will not be integer in general so that more sophisticated schemes will be required to solve the DBMPE.

Now we are ready give some remarks on the connections of the DBMPE (25), the LBM (27) and a general DVM. Essentially, the DBMPE is a specific DVM with carefully chosen discretization in particle velocity space and expansion order for distribution functions so that the conservation laws are satisfied precisely, and then the LBM is a DBMPE with a fixed numerical discretizations Eq. (27) in the physical space \mathbf{r} and time t . In general, the numerical discretizations in \mathbf{r} and t are not specified for the DBMPE, any available discretization techniques in space and time can be applied for Eq. (25) including finite difference/volume/element schemes, which are correspondingly named as finite difference/volume/element LBM in community (see also [10]). In fact, Eq. (27) is a special finite difference scheme. Nevertheless, the DBMPE maintains an important feature of the LBM, i.e., seeking minimal discretization set in the particle velocity space which is guided by satisfying conservation property[8]. Compared with a general DVM, the computational cost is often be reduced. In this work, we focus on the derivation of DBMPE (25) and the impact of truncation of Hermite expansion and the relevant Gauss-Hermite quadrature on the capability for simulating shallow water flows, in particular, supercritical flows.

2.2 Remarks on accuracy of equation (25)

As previously shown, errors are introduced to the DBMPE (25) by truncating equilibrium function and discretizing particle velocity space, i.e., from Eq. (11) to Eq. (23) and from Eq. (23) to Eq. (25).

In principle, if the order of the Hermite expansion is sufficiently high, Eq. (23) is expected to accurately recover Eq. (11). In practice, however, only a few orders may be affordable in term of computational cost, and the approximation accuracy will be determined by the expansion order. In general, the accuracy will be related to the Froude number, i.e., higher Froude numbers may need more expansion terms, cf. Eq. (12) and Eq. (14). For instance, similar to gas dynamics, see Ref. [15], using a first-order expansion leads to a linear equation which is only suitable when $Fr \rightarrow 0$. Specifically, we may introduce a L^2 norm

$$E_T = \sqrt{\frac{\int (f^{eq} - f_{eq}^N)^2 d\mathbf{c}}{\int (f^{eq})^2 d\mathbf{c}}}$$

to measure the difference of f_{eq}^N from f^{eq} over the whole particle velocity space. In Fig. 1, contours of E_T over the macroscopic velocity range of $u \in \{-2.5, 2.5\}$ and $v \in \{-2.5, 2.5\}$ are plotted. For comparison, we consider both the second-order expansion and fourth-order expansion of the equilibrium distribution function. It is also worthwhile to note that E_T represents an accumulation of errors from all discrete velocities so that its value can be large. From these contours, we clearly see that the error grows with increasing macroscopic velocities in general. In comparison to the second-order expansion, the fourth-order expansion leads to smaller error where the speed is relatively small but increases the error quickly with larger speed. When $h = 0.001$, the error grows slower but its magnitude is fairly significant (roughly 1 for both orders of expansions) even with the zero speed.

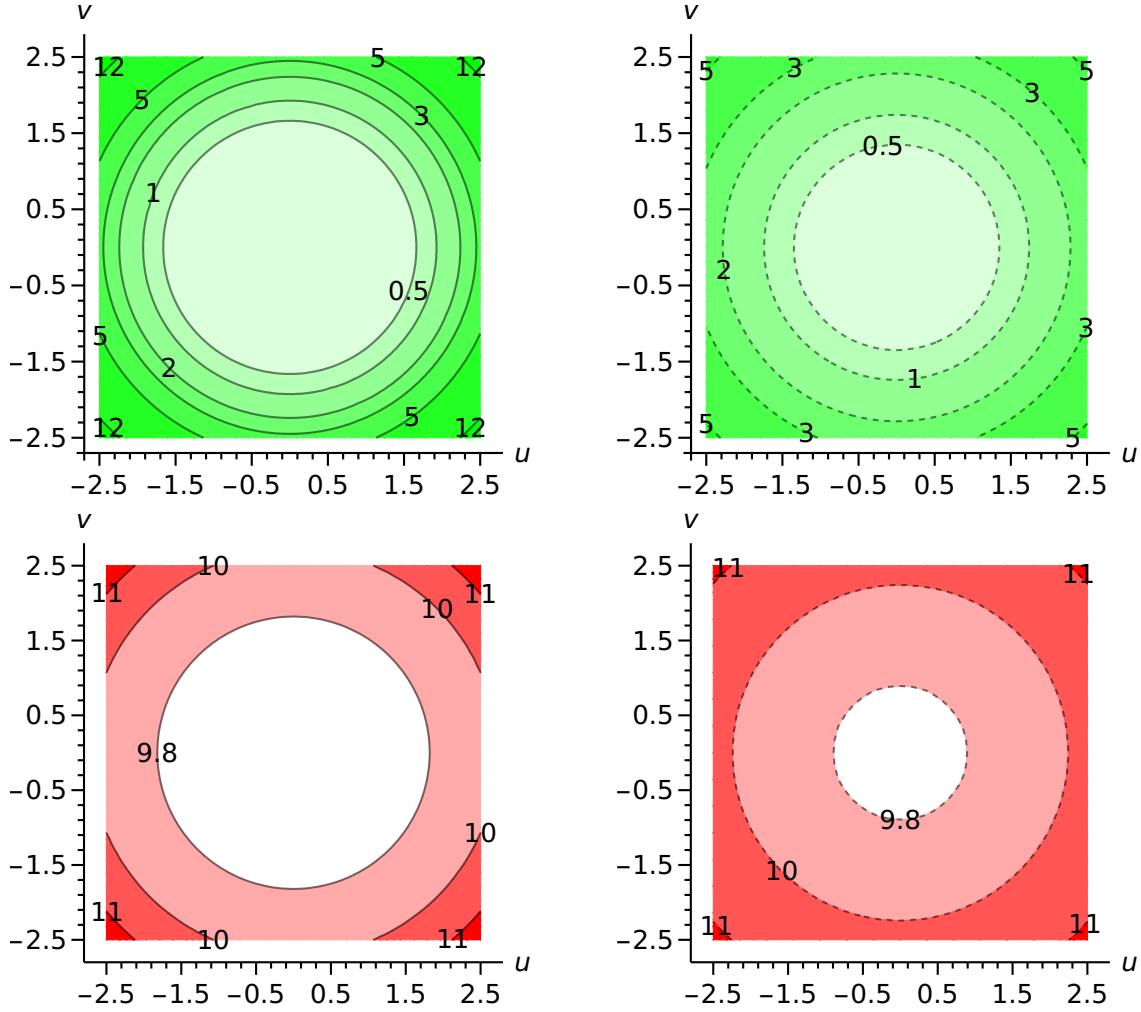


Figure 1: Contours of E_T when the fourth-order (left, solid contour lines) and the second-order (right, dashed contour lines) expansion are used respectively for f_{eq}^N at $h = 1$ (top, green color gradient) and $h = 0.001$ (bottom, red color gradient). To better display the contour labels at $h = 0.001$, the E_T values are transformed by $100(E_T - 0.9)$, which leads to the relationships, $9.8 \rightarrow E_T = 0.998$, $10 \rightarrow E_T = 1$ and $11 \rightarrow E_T = 1.01$.

Overall, the results imply that it is challenge for a DBM to simulate flows with large speed and large depth ratio. However, since the conservation laws are retained naturally, even with limited expansion order, the DBMPE may be sufficient for a broad range of the hydrodynamic problems, particularly if the diffusion term plays a negligible role (e.g., the numerical tests in Sec. 3).

The second kind of error is from the chosen quadrature. According to the Chapman-Enskog expansion, when the “Knudsen” number \mathcal{K} is small, the first-order asymptotic solution of Eq. (23) may be written as

$$f^{(1)} = -\tau(\partial_t^{(0)} + \mathbf{c} \cdot \nabla + \mathbf{F} \cdot \nabla_c)f^{(0)}, \quad (28)$$

where the zeroth-order solution, $f^{(0)}$, is just the truncated equilibrium function, f_{eq}^N . From Eq. (28), $f^{(1)}$ will include a polynomial of \mathbf{c} of one order higher than that in $f^{(0)}$. Therefore, to numerically evaluate the integration of Eqs. (6) to (8), we need a quadrature with the degree of precision

$$P = 2d - 1 \geq N + 1 + M,$$

to calculate the M^{th} order of moment (e.g., $M = 0$ for the zeroth-order moment, h). Specifically,

if using a 4th order Hermite expansion and to get the stress right ($M = 2$), we need at least a quadrature with the 7th order of precision, which may need four discrete velocities in one dimension.

2.3 Remarks on external force term

For modeling shallow water flows, a well-balanced numerical scheme is often desired, which precisely satisfies the steady SWEs at discrete level [16, 2]. For the brevity of discussion, the Euler type equations are often employed in literature, i.e.,

$$\nabla \cdot (h\mathbf{V}) = 0, \quad (29)$$

and

$$\nabla \cdot (h\mathbf{V}^2) + \nabla \mathcal{P} = h\mathbf{F}, \quad (30)$$

where the variables are already normalized using Eq. (10). In this sense, a well-balanced scheme means that the discretization for the RHS and LHS terms of Eq. (30) will be carefully chosen to ensure the validity of Eq. (10) in its discrete form

Here we mainly concern if the truncation on the Hermite expansion and the discretization in the particle velocity space can satisfy the well-balanced property. In other words, if Eq. (25) can recover Eq. (30) under the steady state. For this purpose, we substitute Eq. (15) and Eq. (22) into Eq. (25), multiply both RHS and LHS terms by \mathbf{c} , and integrate them over the particle velocity space. Thus we need to validate if the equation

$$\nabla \cdot \int f_{eq}^N \mathbf{c}^2 d\mathbf{c} = \int \mathcal{F} \mathbf{c} d\mathbf{c}, \quad (31)$$

is equivalent to Eq. (30). We note that the integration and the summation are exchangeable in such as Eq. (16) with sufficiently accurate quadrature. Considering Eqs. (16), (17)-(21) and (22), it is straightforward to obtain that

$$\int f_{eq}^N \mathbf{c}^2 d\mathbf{c} = h\mathbf{V}^2 + \mathcal{P}\delta, \quad (32)$$

and

$$\int \mathcal{F} \mathbf{c} d\mathbf{c} = h\mathbf{F}. \quad (33)$$

Therefore, the discretization in particle velocity space precisely holds the well-balanced property.

For a practical simulation, Eq. (25) has to be further discretized in \mathbf{r} and t and becomes algebraic equations e.g., Eq. (27), which may alter the well-balanced property. As we have no preference for such discretizations in this work, we will leave the discussion open for future works where the relevant schemes are specified. In fact, a few different schemes will be employed in the following to serve the purpose of studying the impact of the Hermite expansion and the corresponding Gauss-Hermite quadrature. Nevertheless, it is possible to realize the well-balanced property for the standard stream-collision scheme, as shown by Zhou [7].

3 Numerical validation

In the following, we will numerically validate if the capability of simulating supercritical flows can be enhanced by using higher order expansion and quadrature. For this purpose, we first need to determine the discretization scheme in space \mathbf{r} and t . Since their impacts are not our focus in this work, we employ a few simple schemes according the type of Hermite abscissae, i.e., the combination of upwind schemes and an Euler forward scheme in time for general discrete velocity sets, and the scheme Eq. (27) for integer velocities. Afterwards, the fully discretized equations are solved for two classical problems, i.e., one-dimensional dam-break problem and two-dimensional circular dam-break problem.

By utilizing Eq. (15), the Hermite abscissae and Eq. (24), it is straightforward to construct various discrete velocity sets. For instance, to simulate high Froude number flows, we may need to use a fourth order expansion for f_{α}^{eq} and a quadrature of at least 7th order of precision, see discussions in

Sec. 2.2. By contrast, if the flow is subcritical, then it may be enough to employ commonly used nine-velocity set and a second order expansion for f_α^{eq} . When the fourth expansion terms are employed for f_α^{eq} , we use a set of 16 discrete velocities obtained from the roots of fourth order Hermite polynomial. These 16 discrete velocities are not integer and require a finite difference scheme. For convenience, we list the roots of the fourth-order Hermite polynomial in one-dimensional space in Table 1. The two-dimensional 16-velocity set can then be constructed by using the “production” formulae. The two dimensional 9-velocity set is commonly used so that the detail is ignored here.

Table 1: Quadrature from the fourth-order Hermite polynomial. The two-dimensional set can be constructed by using the “production” formulae, i.e., $\mathbf{c}_\beta = (c_i, c_j)$ and $w_\beta = w_i w_j$ where $\beta \in \{0..15\}$ and $i, j \in \alpha$.

α	Roots (c_α)	Weights (w_α)
0	$-\sqrt{3 - \sqrt{6}}$	$\frac{12}{\left(6\sqrt{2(3-\sqrt{6})} - 2\sqrt{2(3-\sqrt{6})}^{3/2}\right)^2}$
1	$\sqrt{3 - \sqrt{6}}$	$\frac{12}{\left(6\sqrt{2(3-\sqrt{6})} - 2\sqrt{2(3-\sqrt{6})}^{3/2}\right)^2}$
2	$-\sqrt{3 + \sqrt{6}}$	$\frac{12}{\left(6\sqrt{2(3+\sqrt{6})} - 2\sqrt{2(3+\sqrt{6})}^{3/2}\right)^2}$
3	$\sqrt{3 + \sqrt{6}}$	$\frac{12}{\left(6\sqrt{2(3+\sqrt{6})} - 2\sqrt{2(3+\sqrt{6})}^{3/2}\right)^2}$

For the one-dimensional dam-break problem, we set the whole domain to be 1000 in the non-dimensional system (i.e., $1000h_l$ in the dimensional system while the initial depth h_l at the inlet is chosen as the reference length). An initial discontinuity will be placed at the middle $x = 500$ (see Fig. 2). For supercritical flow, the initial water depth is 1 at the left half domain (i.e., the reference length scale) and 0.001 at the right half, while for the subcritical case, the ratio is 1 : 0.25.

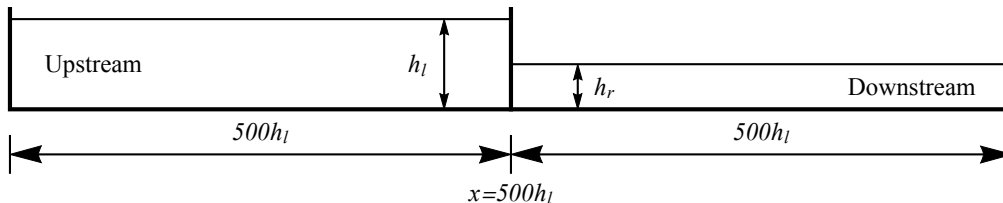


Figure 2: Configuration of the one-dimensional dam-break problem at the initial time (not to scale).

To test the supercritical flow, the parameters for calculation are chosen as $\mathcal{K} = 0.001$, $dx = 0.5$, and $dt = 0.0001$, and the 16-velocity set is employed with the fourth-order expansion. Since the quadrature is non-integer, a first-order upwind scheme is chosen for the space discretization. The results at $t = 150$ and $t = 200$ are shown in Fig. 3. Excellent agreement is found for both water depth and velocity with the analytical solution [17], although numerical error is found for the profile of local Froude number at the position of discontinuity due to the phase lag between water depth and velocity caused by numerical diffusion of upwind schemes [10]. The simulation confirms the capability of modeling supercritical flows with a fourth order expansion and corresponding quadrature. By contrast, we also tested the combination of a second-order expansion and 16 discrete velocities, but found that the simulation is unstable using the same problem setup.

For the subcritical flow, we use the stream-collision scheme (27) and the parameters are chosen as $\mathcal{K} = 0.1$, $dx = 0.5$, and $dt = dx/\sqrt{3}$. The numerical results are shown in Fig. 4, where excellent agreement with the analytical solutions [17] can be found. Moreover, it appears that there is almost no numerical diffusion, which is consistent with the property of the scheme (27). However, possibly due to this property, the capability in simulating supercritical flows is limited. By using a multispeed

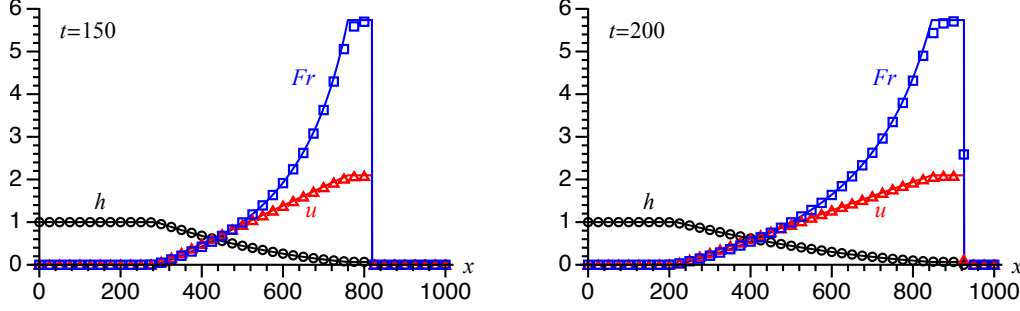


Figure 3: Profiles of depth, velocity and local Froude number for the one-dimensional dam-break problem with $h_l : h_r = 1000 : 1$. Lines and symbols represent analytical and numerical solutions, respectively.

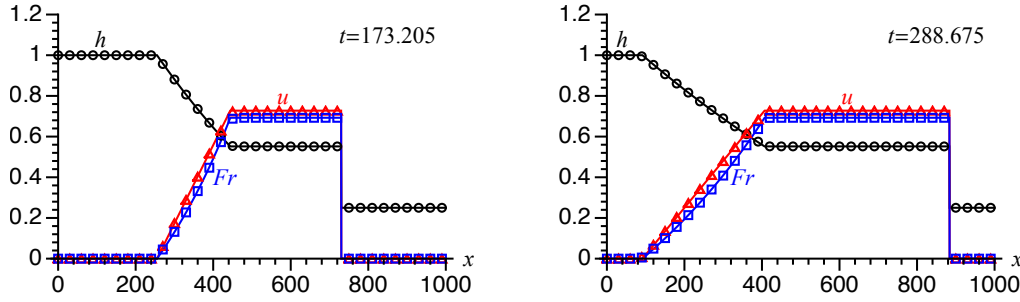


Figure 4: Profiles of depth, velocity and local Froude number for the one-dimensional dam-break problem with $h_l : h_r = 4 : 1$. Lines and symbols represent analytical and numerical solutions, respectively.

lattice with 37 integer discrete velocities together with a fourth order expansion for the equilibrium function, we observe instability when the ratio is $h_l : h_r = 20 : 1$ using the stream-collision scheme, which confirms the findings of Peng et al.[18] However, an appropriate finite difference scheme can still maintain stable simulations.

To further test the capability of the DBMPE, we employ a two-dimensional circular dam-break problem. In this case, a cylinder water column with height h_c and radius r_c is set in the initial time and start to collapse with the time. For the benchmark purpose, we choose the problem setup given by Billett and Toro[19], where the flow is transcritical. As shown in Fig. 5, by choosing h_c as the reference length, the computational domain is a 2×2 square, and the initial radius of water column is set to be $r_c = 0.35$ while the water depth in other area is set to be 0.1. In numerical simulations, the set of 16 discrete velocities is employed together the fourth-order expansion for the equilibrium function. To adapt to the non-integer quadrature, we use a second-order upwind scheme in space for this case, while the parameters for calculation are chosen as $\mathcal{K} = 0.001$, $dx = dy = 0.005$, and $dt = 0.0001414$.

In Fig. 6, the profiles of depth and local Froude number at the x-strip $y = 1$ are compared with those obtained by Billett and Toro [19] using a finite volume scheme with the van Leer limiter. As has been shown, two sets of numerical results agree well with each other. In the comparison, we notice the differences of the non-dimensional system between two works. In particular, the "Fr" defined in [19] is actually Fr^2 in this paper. In Fig. 7, we also show the depth profiles for the whole domain. Clearly the higher order expansion and quadrature help in simulating supercritical flows.

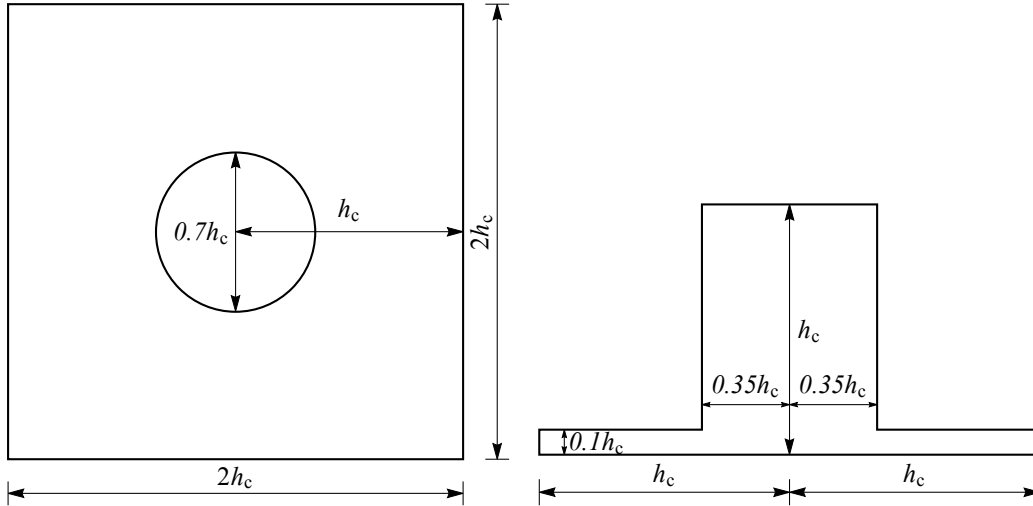


Figure 5: Configuration of the 2D circular dam-break problem, left - top view, and right - side view. The illustrations are not to scale.

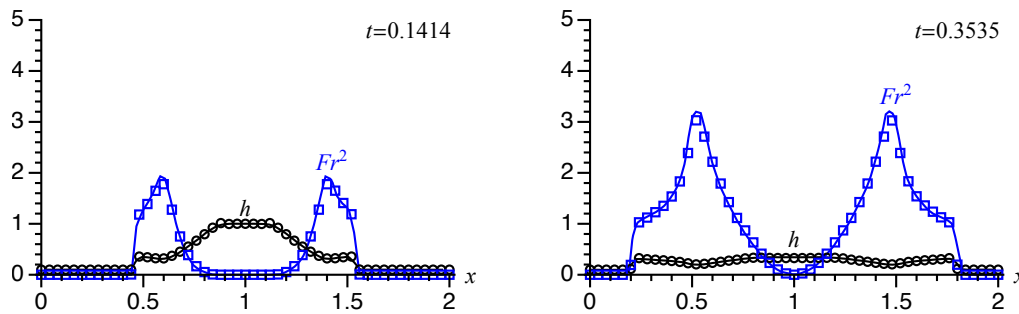


Figure 6: Profiles of depth and the square of local Froude number at the x -strip $y = 1$ for the circular dam-break problem. Lines and symbols represent reference solutions present in [19] and the present numerical solutions, respectively.

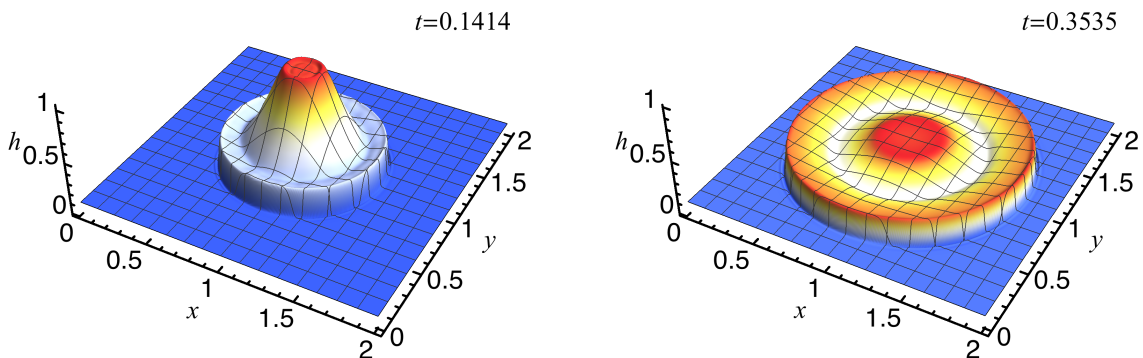


Figure 7: Depth profiles for the 2D circular dam-break problem. The coordinate lines are shown in the plots.

4 Concluding remarks

To summarize, we have derived a type of discrete Boltzmann model with polynomial equilibria for simulating shallow water flows. Utilizing the Hermite expansion and the Gauss-Hermite quadrature, the DBMPE naturally satisfies the conservation property of the collision integral, which greatly simplifies the algorithm. We also discussed the impact of truncating distribution functions and discretizing particle velocity on the accuracy of DBMPE, and give indications on choosing the expansion order and quadrature according to the requirement of problems, e.g., *Fr*. In particular, if the quadrature consists of integer abscissae, we can obtain the very simple and efficient lattice Boltzmann scheme. Moreover, we found that there is no sacrifice in the well-balanced property for treating the source term. Further numerical validations for the one-dimensional dam-break problem and the two-dimensional dam-break show that the capability of simulating supercritical flows is enhanced by increasing the expansion and quadrature order.

By providing the flexibility on deriving both the single-speed DBM suitable for the stream-collision scheme, and various high-order DBMs, we expect that the applications of these models range from subcritical flows to supercritical flows. In the near future, we will further study those applications concerning supercritical flows. There are also fundamental questions remaining open, e.g., how to achieve a well-balanced scheme if taking the discretization in space and time into account, in particular for high-order models where general finite difference schemes are required.

Acknowledgements

Authors from the Daresbury laboratory would like to thank the Engineering and Physical Science Research Council (EPSRC) for their support under projects EP/P022243/1 and EP/R029598/1. Authors from the Sichuan University would like to thank the support of the National Natural Science Foundation of China under grant numbers: 51579166 and 5151101425.

References

- [1] M. S. Ghidaoui, J. Q. Deng, W. G. Gray and K. Xu, *Int. J. Num. Methods Fluids* **35**, 449 (2001).
- [2] K. Xu, *J. Comput. Phys.* **178**, 533 (2002).
- [3] J. H. Liang, M. S. Ghidaoui, J. Q. Deng and W. G. Gray, *J. Hydraul. Res.* **45**, 147 (2007).
- [4] P. Prestininzi, M. L. Rocca, A. Montessori and G. Sciortino, *Comput. Math. Appl.* **68**, 439 (2014).
- [5] J. G. Zhou, *Int. J. Mod. Phys. C* **13**, 1135 (2002).
- [6] J. G. Zhou, *Comput. Methods App. Mech. Eng* **191**, 3527 (2002).
- [7] J. G. Zhou, *Lattice Boltzmann methods for shallow water flows* (Springer, Berlin, 2004).
- [8] S. Chen and G. D. Doolen, *Annu. Rev. Fluid Mech.* **30**, 329 (1998).
- [9] B. Chopard, V. Pham and L. Lefèvre, *Comput. Fluids* **88**, 225 (2013).
- [10] M. L. Rocca, A. Montessori, P. Prestininzi and S. Succi, *J. Comput. Phys.* **284**, 117 (2015).
- [11] X. W. Shan, X. F. Yuan and H. D. Chen, *J. Fluid Mech.* **550**, 413 (2006).
- [12] X. Shan and X. He, *Phys. Rev. Lett.* **80**, 65 (1998).
- [13] W. Y. Tan, *Shallow water hydrodynamics : mathematical theory and numerical solution for a two-dimensional system of shallow water equations* (Water & Power Press, China and Elsevier, Amsterdam 1992).
- [14] H. Grad, *Commun. Pure Appl. Math.* **2**, 331 (1949).

- [15] J. Meng and Y. Zhang, *J. Comput. Phys.* **230**, 835 (2011).
- [16] S. Noelle, Y. Xing and C.-W. Shu, High-order Well-balanced Schemes, in *Numerical Methods for Balance Laws*, quaderni di matematica (Aracne, November 2010), p. 364.
- [17] O. Delestre, C. Lucas, P.-A. Ksinant, F. Darboux, C. Laguerre, T. N. T. Vo, F. James and S. Cordier, *Int. J. Numer. Meth. Fl.* **72**, 269 (2013).
- [18] Y. Peng, J. P. Meng and J. M. Zhang, *Mathematical Problems in Engineering* **2017**, p. 5 (2017).
- [19] S. J. Billett and E. F. Toro, *J. Comput. Phys.* **130**, 1 (1997).